Pharm Res (2011) 28:640–646
DOI 10.1007/s11095-010-0317-1

RESEARCH PAPER

Molecular Interaction Fields (MIFs) to Predict Lipophilicity and ADME Profile of Antitumor Pt(II) Complexes

Giulia Caron • Mauro Ravera • Giuseppe Ermondi

Received: 29 August 2010 / Accepted: 1 November 2010 / Published online: 17 November 2010

ABSTRACT

Purpose To describe a computational tool to calculate molecular descriptors of potential application in ADME virtual screening of antitumor Pt(II) drug candidates.

Methods The multistep computational procedure consists in (a) building and optimization (PM3) of the 3D structures of the investigated complexes, (b) parametrization of Pt(II) and its implementation in GRID, (c) GRID calculations and extraction of the information content with VolSurf and BIOCUBE4mf, and (d) PLS analysis to look for the correlation between experimental data and the molecular descriptors.

Results The following results were obtained: (a) the calibration of the GRID force field to take into account the platinum di-cation, (b) solid PLS models between log k30 and log kw with VolSurf descriptors which highlight the main structural differences between the two chromatographic parameters, (c) the prediction of virtual (of each conformer) log k30 and log kw, and (d) the identification of the main descriptors governing VD_{ss} of drugs in clinical use.

Conclusion The study suggests a strategy to identify good Pt (II) complexes prior to their synthesis to eliminate as soon as possible drug candidates with unfavorable PK profile.

Electronic Supplementary Material The online version of this article (doi:10.1007/s11095-010-0317-1) contains supplementary material, which is available to authorized users.

G. Caron • G. Ermondi (✉)
CASSMedChem Research Group, DSTF at the Centre for Innovation
Università di Torino
Via Quarello 11
10135, Torino, Italy
e-mail: giuseppe.ermondi@unito.it

M. Ravera
Dipartimento di Scienze dell'Ambiente e della Vita
Università del Piemonte Orientale "Amedeo Avogadro"
Viale Michel 11
15121, Alessandria, Italy

KEY WORDS ADME prediction · distribution volume · lipophilicity · Molecular Interaction Fields · Pt(II) complexes

INTRODUCTION

Platinum drugs are now established as effective anticancer agents (1,2). The severe systemic toxicity and drug resistance of cisplatin and its analogues has stimulated the quest for new platinum-based compounds obtained by modifying the ligands around the metal centre. In particular, complexes that (a) display different DNA-binding modes (non-classical platinum complexes), (b) are activated only in the tumour tissue, and (c) are accumulated at the tumour site by virtue of an accurate active and/or passive drug targeting and delivery strategy have recently been proposed to improve clinical effect (3). However, up-to-date drug design strategies aimed at finding new Pt (II)-based anticancer agents do not include either Drug Metabolism and Pharmacokinetics (DMPK) or physico-chemical virtual screening. The prediction of the ADME profile of new Pt(II) complexes could indicate good complexes prior to their synthesis to eliminate drug candidates with unfavorable PK profile as quickly as possible, thus limiting animal experimentation as well (4).

Pt(II) complexes represent a dataset of not easy integration in larger databases of organic compounds and, thus, of difficult comparison with standard pharmaceutical products. For example, the peculiar chemical properties of Pt(II) complexes require very particular chromatographic conditions to obtain lipophilicity data, far from those that may be applied to organic molecules. In addition, the traditional shake-flask method suffers from significant errors caused by the very negative lipophilicity values generally related to such a class of compounds.

Some computational methods were shown to be able to calculate lipophilicity of Pt(II) complexes (5), but none of them was designed (a) to calculate virtual lipophilicity (of each conformer) and (b) to predict chromatographic retention indexes which represent the best suited descriptors for this class of compounds. In fact, the measurement of lipophilicity descriptors for Pt(II) complexes are dependent on the already mentioned chemical properties, handling and toxicity of compounds. Chromatographic determination of retention indexes (i.e. the RP-HPLC isocratic and the extrapolated retention factors, log k30 and log kw (6,7)) are generally more convenient than shake-flask experiments measuring log P/log D and can also provide relevant information about the compound's property even without conversion in log P (8).

In this study, we first report the setting-up of an *in silico* tool based on GRID/VolSurf software to predict virtual (of each conformer) chromatographic retention factors (log k30 and log kw) for Pt(II) complexes of potential antitumor activity. The method is based on the parametrization of Pt(II) into GRID force field (9–11) that can be used either alone or implemented in GRID-based software (e.g. VolSurf, ALMOND, MetaSite (12)). In particular, here we used VolSurf 2D descriptors, since these latter quantitatively characterize polarity and hydrophobicity, which are the main factors governing lipophilicity (13), and we already used them to calculate virtual $\log P^{N}_{alk}$ of molecules in the alkane/water system (14,15).

The prediction of the steady-state volume of distribution (VD_{ss}) is a key step in ADME profiling of drug candidates, since VD_{ss} together with clearance determines the half-life and, thus, impacts on the dosing regimen of a compound (16). Lipophilicity and MIFs-derived descriptors were proven to be relevant in predicting VD_{ss} of large compounds datasets (17), thus, in the second part of the paper we verified whether the same was true for the small series of Pt(II) drugs in clinical use. Results suggested the relevant role played by the hydrogen bond acceptor (HBA) properties of complexes in governing their VD_{ss} and the negligible contribute of lipophilicity.

METHODOLOGY

The 3D structures of investigated Pt(II) complexes were obtained by modification of the X-ray structure of five complexes deposited in the Cambridge Structural Database (http://www.ccdc.cam.ac.uk/products/csd/) (see "Supplementary Material" for details). The crystal structures were imported in Spartan '08 molecular modeling software (http://www.wavefun.com/) and modified with the builder tool when necessary. According to literature (18), the geometry of the complexes was fully optimized without symmetry constraints using the semiempirical quantum-mechanical PM3 Hamiltonian as implemented in Spartan '08 and retained for GRID v22.b (http://www.moldiscovery.com/) calculations. For flexible compounds, additional conformations were generated with Spartan '08 with the standard analysis conformational tool and ranked according to their heat of formation (kcal/mol).

The final structures were saved in mol2 and submitted to GRID to obtain MIFs. The readable .kont files were analyzed with the help of BIOCUBE4mf v1.01 (http://www.casmedchem.unito.it/), whereas the binary .kont files of all structures were submitted to VolSurf v.4.1.2 software (http://www.moldiscovery.com/) for the calculation of the MIFs-derived descriptors (92, extracted from MIFs obtained with the OH2, DRY, N1 and O probes).

PLS analysis tools was used as implemented in the VolSurf v.4.1.2 software. In addition, XLStat v.2009.6.04 (www.xlstat.com) was employed to obtain the VIP plots.

RESULTS AND DISCUSSION

In this study, a series of Pt(II) derivatives ($n=24$) reported by Platts *et al.* (19) was selected as a reliable dataset of lipophilicity indexes, since the experimental procedure to obtain log k30 values (log k30 ranges from −0.73 to 0.98 and corresponds to a variation in log P_{oct} from −2.22 to 1.13 according to the reported calibration curves (19)) was clearly referenced (20) and of high experimental quality. The full list of structures and data is in the "Supplementary Material".

Before submitting Pt(II) complexes to VolSurf to calculate molecular descriptors, it was necessary to calibrate the GRID force field to take into account the platinum di-cation. Usually, the check and the refinement of the GRID force field is based on the calculation of GRID maps for high resolution ligand-macromolecule X-ray structures. In particular, the correctness of the calibration is evaluated by comparing the position of the ligand atoms with the GRID maps obtained with different probes. Since Pt(II) complexes are bound covalently to nucleotides, in this case it is not possible to calibrate the force field on the basis of Pt(II) position. Instead, we used the position of water molecules extracted from a high resolution cisplatin-DNA structure deposited in the PDB (PDB code: 1I1P, (21,22)) with an accurate determination of water molecules caged around ligand (cisplatin). In particular, according to Pastor *et al.* (23), we assumed that the presence of any water molecule in its observed crystallographic position was energetically favorable. In practice, we used GRID to calculate the MIFs for the water probe and BIOCUBE4mf (24) to select the regions satisfying energetic criteria (energy threshold). Results are shown in Fig. 1: the experimental position of the

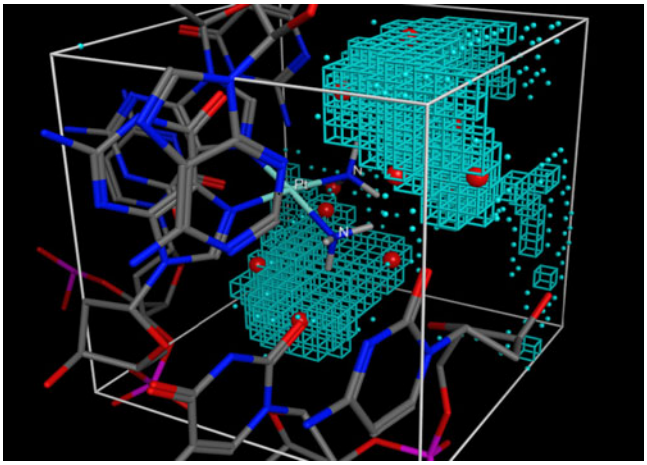

Fig. 1 Validation of Pt(II) parametrization introduced in GRID force field: in *red* the crystallographic position of the water molecule (PDB code: 111P), in *light blue* the clusters of lowest energy calculated by GRID combined with BIOCUBE4mf.

water molecules (red dots) is well reproduced by the clusters of lowest energy (in blue, energy threshold = −3.0 kcal/mol) calculated by GRID. In particular, experimental water molecules form a cage which surrounds the platinum centre. The MIF due to the water probe correctly predicts two favorable locations on both sides of cisplatin along its quaternary axis. These two positions are expected to vary considerably with force field parametrization. Similar results were also found for two additional crystallographic structures (1LU5 and 3CO3, see "Supplementary Material").

A relationship between experimental log k30 and the VolSurf descriptors was obtained by PLS technique (model 1). A 3LVs model was found: the three main components explained about 85% of the total variance ($r^2 = 0.85$). The internal predictive capability of the model ($q^2 = 0.44$) was evaluated using the cross-validation technique (CV) and, in particular, the leave-one-out (LOO) procedure. Complete statistics of model 1 are in Table I. The relationship between experimental and calculated values ($r^2 = 0.85$) is shown in Fig. 2A. A slope of about 1 and an intercept of about 0 indicate a very good correspondence between experimental and calculated values.

The external predictive skills of the PLS method were evaluated with an external test set of eight Pt(II) complexes (chemical structures are in "Supplementary Material"). **TS1** and **TS2** are complexes bearing pyridine moieties (see "Supplementary Material" for details about their preparation), whereas **TS3**-**TS8** are a series of cis-diamminemalonatoplatinum(II) derivatives recently described in literature (18). Test set experimental lipophilicity data (Table II) were obtained with the same method used for measuring log k30 of the training set (18). Predictions were first calculated on the fully optimized conformer (PM3 column in Table II), and a generally good match between experimental and calculated log k30 was found, except for **TS7** and to a smaller extent, for **TS5**, which were predicted more hydrophilic than expected. Even though the difference between experimental and calculated values for these two complexes was not dramatic (less than 0.4), we decided to investigate whether conformational effects could be related to this finding, as described in the details below, after analyzing the model for its chemical interpretability. To obtain a correct chemical interpretation of a PLS model, it is necessary to carefully inspect the variable importance in the projection (VIP) plot together with the PLS coefficients (14). Briefly, the VIPs show which descriptors are the most important for the model, whereas the sign of the PLS coefficients indicates the positive or negative contribution of the descriptor to the investigated variable. Fig. 3 shows the VIPs plot of model 1 in red (the full list of VIPs together with their values and signs is in the "Supplementary Material"). As expected, the most relevant contributions to log k30 (VIPs >1.5) were given by the hydrophobic (D1-, D2-, D3-DRY, on the left) and size/shape descriptors (S, V-OH2, on the right). Their definition is available in the "Supplementary Material". All of them had PLS positive signs; thus, the larger they were, the larger log k30 was and, consequently, the more lipophilic the complex.

The training set contains rigid and semirigid structures except for **22** (and **24** to a lesser extent) and, thus, is poorly affected by molecular flexibility. Conversely, the test set contains six flexible complexes (**TS3-TS8**). In a recent paper (14), we suggested a strategy to handle virtual log P of flexible compounds where the first step is the building of an averaged conformer (i.e. a reasonably averaged 3D structure). This step is not a trivial procedure for Pt(II) complexes (for organic molecules one could use common

Table I PLS Models Discussed in the Paper

Model	Exp	Number of observations, *n*	Number of latent variables, LV	Cumulative determination coefficient, r^2	Cross-validated correlation coefficient, q^2	Root mean square of the errors, RMSE
1	log k30	24	3	0.85	0.44	0.16
2	log kw	24	3	0.88	0.57	0.29

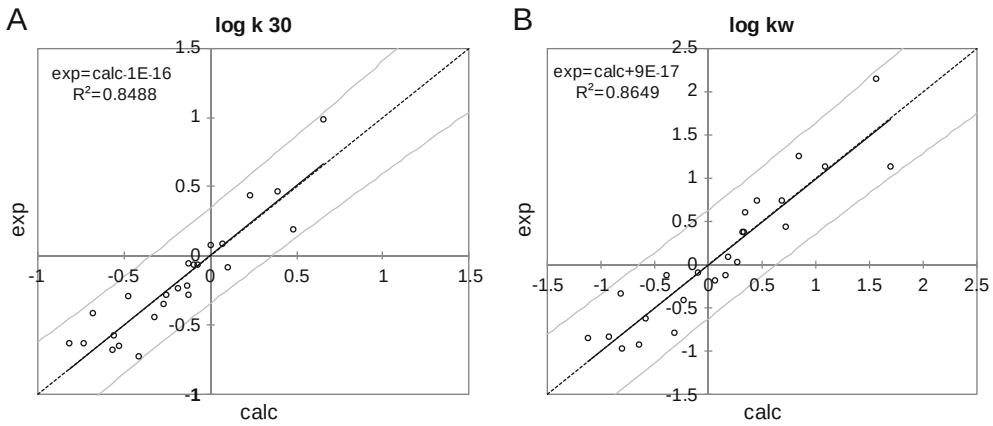

Fig. 2 Correlation between experimental (*exp*) and calculated (*calc*) RP-HPLC-based lipophilicity indexes: **A** log k30; **B** log kw.

algorithms such as Omega, CONCORD or CORINA), and in this study we decided to replace the averaged conformer with the fully optimized conformer. In practice, after some assays, we decided to use PM3 as the minimization algorithm (see "Methodology") which produced rather folded averaged conformers for the whole test set (Fig. 4A for **TS7**). As mentioned above, the virtual log k calculated for these conformers matched experimental values well except for **TS5** and **TS7**. To check which conformer better reproduces experimental values, we submitted the whole test set to conformational analysis, and virtual log k30 was calculated for every conformer. Interestingly, the log k30 lipophilicity range (the difference in log k30 between the most lipophilic and the most hydrophilic conformer) was about 0.5 (comparable with a log P_{oct} range of about 1 unity according to calibration curves reported by Platts *et al.* (19)). The conformational analysis of **TS7** produced, among others, a number of extended conformations; the most stable of them (**TS7***) is reported in Fig. 4B, and its calculated virtual log k30 (0.27) is close to the experimental value (0.19). The same is true for **TS5**. The similar behavior of **TS5** and **TS7** cannot be clearly deduced from the comparison of their chemical structures.

Since size/shape and hydrophobic contributions mainly govern the variation in log k30 as described above, we verified whether these descriptors were able to explain the differences in lipophilicity between **TS7** and **TS7***: **TS7** is folded, and, thus, its shape is different from **TS7***, which shows an extended conformation. Moreover, the points of the MIF due to the DRY probe (in yellow in Fig. 4), calculated with BIOCUBE4mf (24) at −0.5 kcal/mol, are a good approximation of the VolSurf D descriptors (the hydrophobic descriptors) and strongly vary between the two conformers, both in location and in number, being 330 for **TS7** and 528 in **TS7***. These findings also support the reliability of the chemical significance of the PLS model.

In a recent study, we successfully demonstrated the skills of this approach based on an overall analysis of VIPs profile generated by the same VolSurf descriptors used here (14) to distinguish two widely-known lipophilicity indexes ($\log P^{N}_{oct}$ and $\log P^{N}_{alk}$). Since the paper of Platts *et al.* (19) also reports log kw data for the 24 complexes, we verified whether the approach here described is able to distinguish in an interpretable way the two chromatographic indexes.

Table II External Test Set Prediction

Compound	log k30 (Exp)[a]	log k30 (Calc)			
		PM3[b]	Max[c]	Min[d]	Lipophilicity range[e]
TS1	0.15	0.07	–	–	–
TS2	0.64	0.47	–	–	–
TS3	−0.67	−0.69	−0.69	−1.03	0.34
TS4	0.12	0.01	0.01	−0.17	0.18
TS5	0.11	−0.17	0.01	−0.52	0.53
TS6	0.21	0.20	0.20	−0.21	0.41
TS7	0.19	−0.29	0.27	−0.30	0.57
TS8	0.09	0.20	0.38	−0.16	0.54

[a] experimental value; [b] log k30 calculated on the fully optimized conformer (PM3, see "Methodology"); [c] log k30 of the most lipophilic conformer; [d] log k30 of the most hydrophilic conformer; [e] difference between the most lipophilic and the most hydrophilic conformer

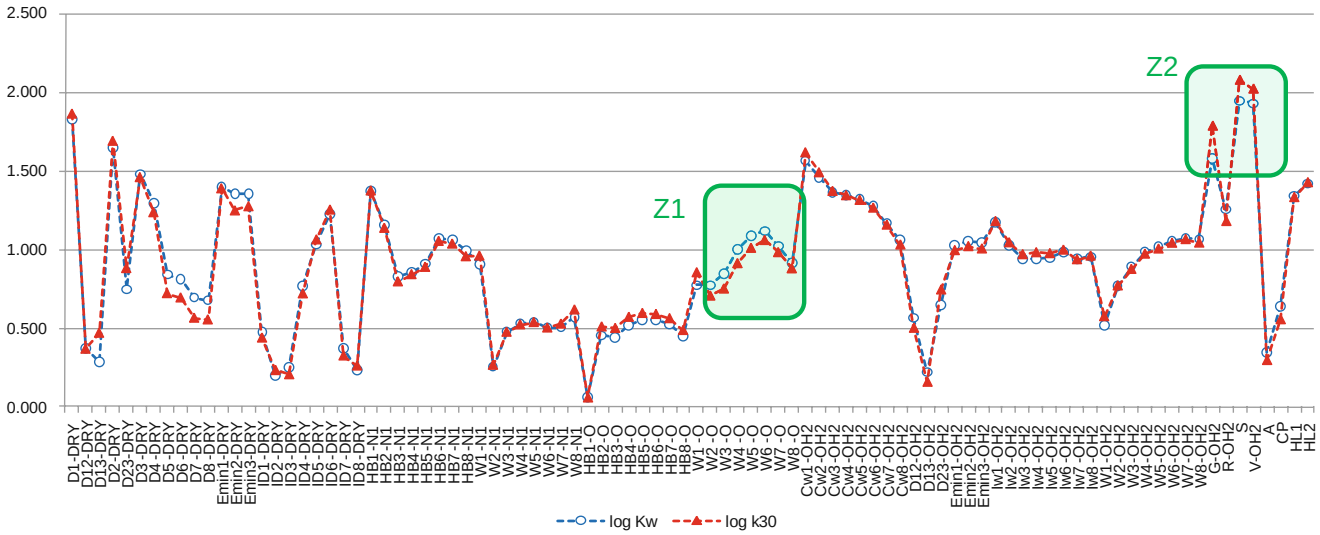

Fig. 3 The VIPs plot for model 1 (log k30, in *red*) and model 2 (log kw, in *blue*). See text for more explanations.

As expected for the investigated series of 24 compounds, log kw and log k30 were highly correlated (Fig. 5) but not superposable, since at different ratios of solvent/water in the mobile phase, the nature of both mobile and stationary phases was modified. In particular, methanol showed more hydrophobic character and lower hydrogen-bond capacity than water. This could cause, at high methanol concentrations, other polar interactions with the stationary phase (25).

To check the ability of our method to detect the differences between the two chromatographic indexes, a relationship between experimental data (here log kw) of the investigated series of 24 Pt(II) complexes and the VolSurf descriptors was again explored by a PLS run. Statistical results are summarized in Table I (model 2) and are slightly better than those obtained for log k30. The relationship between experimental and calculated values is shown in Fig. 2B, where no outliers were identified.

The VIPs plot for model 2 is reported in blue in Fig. 3 and shows that model 2 is, as expected, also due to size/shape and hydrophobic contributions. Fig. 3 suggests that model 1 (log k30) and model 2 (log kw) are similar but not identical. In fact, the two models differ in two regions (Z1 and Z2) where VIPs values are relevant (>1). In particular, Z1 evidences that HBD properties of the solutes are more relevant for log kw, and this is in line with the major water content of the system. Z2 highlights the larger importance of size/shape contributions to log k30; this is in line with the larger hydrophobicity of methanol compared to

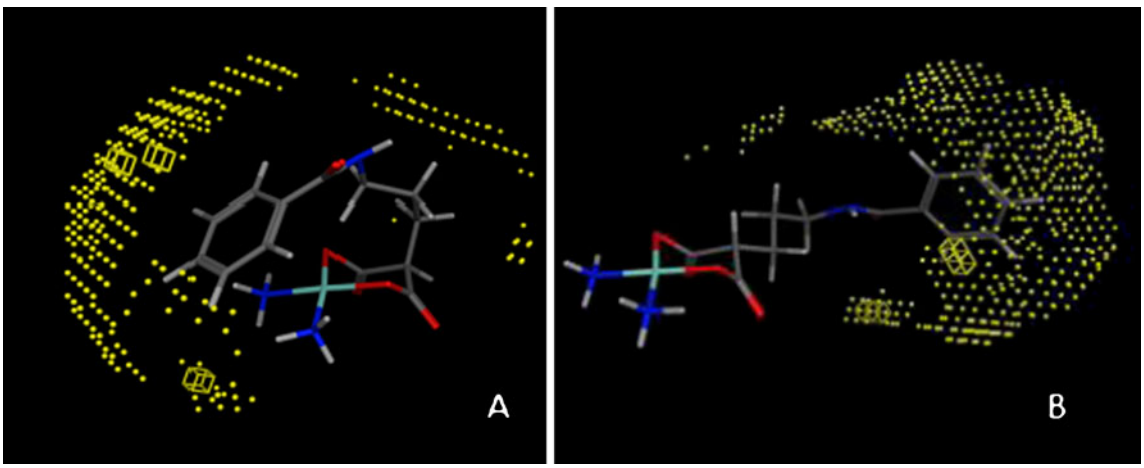

Fig. 4 Two conformers of **7** with different virtual log k30: **A** conformer with minimum energy, **7**; **B** conformer with the best predicted log k value, **7***. The MIF generated by the DRY probe at −0.5 kcal/mol is shown in *yellow*.

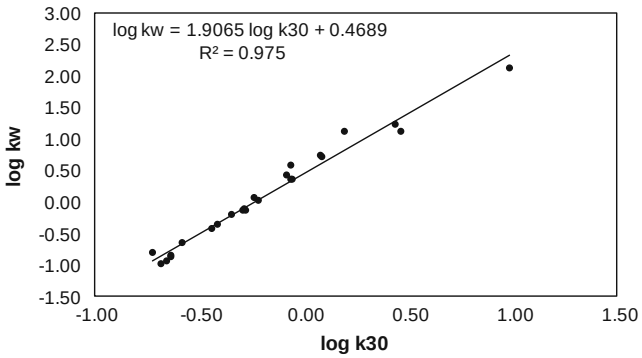

Fig. 5 The correlation between log kw and log k30 for the 24 investigated Pt(II) complexes.

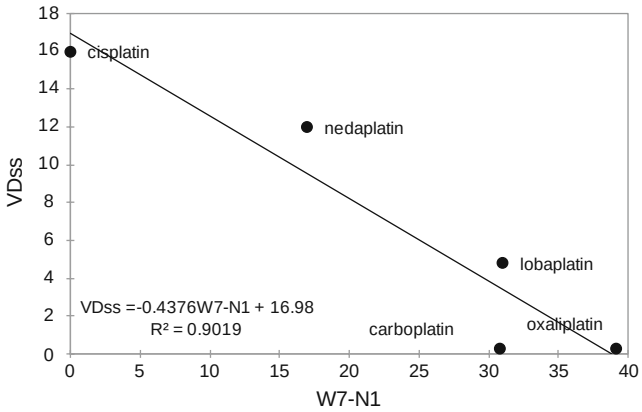

Fig. 6 The correlation between VD_{ss} and the VolSurf descriptor W7-N1 (see text for definition).

water. These findings confirm the method's ability to detect the differences between similar lipophilicity systems.

Volume of distribution, expressed according to Obach *et al.* (16) as the steady-state volume of distribution (VD_{ss},), is a major pharmacokinetic determinant. For large databases of traditional drugs, it was found that VD_{ss} showed trends with some physicochemical descriptors such as clogP, PSA, number of H-bond acceptors and donors, and charge type (16). We thus collected VD_{ss} for Pt(II) drugs used in clinical practice (carboplatin, cisplatin, lobaplatin, nedaplatin and oxaliplatin, all data in "Supplementary Material") (16,26–29) and checked for the molecular descriptors which better correlate with VD_{ss} values. First, in accordance with Lombardo *et al.* (30,31) we consider lipophilicity expressed as log k30 and calculated as described above. No relationship between log k30 and VD_{ss} was found (the same was true for log kw, data not shown). In literature, VD_{ss} values often showed trends with lipophilicity (16), but this is verified for large data sets of unrelated structures and less probable for a small series of analogues as Pt(II) derivatives. A correlation matrix including all VolSurf descriptors and log k30 and log kw was then calculated and showed that many parameters due to the probe N1 and, thus, to the hydrogen bond acceptor (HBA) properties of the Pt(II) complex were related to VD_{ss}. Fig. 6 shows the linear dependence between VD_{ss} and W7-N1, which can be defined as the molecular envelope generating attractive H-bond acceptor interactions computed at −5 kcal/mol. This relationship, which individuates HBA properties as the major determinants for VD_{ss} of Pt(II) complexes, is of practical interest, since it is expected to be used for the design of new series of Pt(II) drug candidates. In practice, to design Pt(II) complexes with high VD_{ss}, chemists should lower the number of HBA moieties, whereas to decrease VD_{ss} the reverse is true. Finally, we tried to look for a correlation between VolSurf molecular descriptors and clearance. Unfortunately, clearance data available in literature suffer from inconsistency since they are expressed in quite different units of measurement, which limits the number of usable values.

CONCLUSION

Pt(II) complexes represent a peculiar class of drugs which are difficult to compare with standard organic pharmaceutical products and require ad hoc *in silico* tools to be used during the various steps of the drug discovery process.

This study shows how the implementation of Pt(II) parameters into GRID force field overcomes one of the main limitations of GRID due to the missing parametrization of some ions. In addition, it enables the separate prediction of retention factors log k30 and log kw for Pt(II) complexes, the more common lipophilicity indexes reported for this class of molecules of potential antitumor activity. Since the method is based on MIFs, it also facilitates checking the dependence of lipophilicity on conformational effects (virtual log k30) as already reported for traditional log P and log D descriptors (virtual log P and virtual log D, respectively).

In addition to lipophilicity, the parametrization of Pt (II) in the force field also enables the calculation of a number of descriptors largely adopted to predict the ADME profiles of compounds. In particular, this study indicates the HBA properties of complexes as the main determinants of VD_{ss} of the five platinum drugs in clinical use and, thus, represents the first step toward the prediction of pharmacokinetic descriptors to be used for screening purposes in new drug design campaigns of Pt(II) antitumor candidates.

The next steps of the study, which are in progress in our laboratories, consist in extending the GRID parametrization to another class of Pt complexes containing the metal atom in the oxidation state IV and in some technical adjustments to automatize and, thus, speed-up calculations.

REFERENCES

1. Kelland L. The resurgence of platinum-based cancer chemotherapy. Nat Rev Cancer. 2007;7(8):573–84.
2. Kelland L, Farrell N. Platinum-based drugs in cancer therapy. Totowa: Humana Pre; 2000.
3. Gabano E, Ravera M, Osella D. The drug targeting and delivery approach applied to Pt-antitumour complexes. A coordination point of view. Curr Med Chem. 2009;16(34):4544–80.
4. Gaviraghi G, Barnaby RJ, Pellegatti M. In: Testa B, van de Waterbeemd H, Folkers G, Guy R, editors. Pharmacokinetic challenges in lead optimization. Zurich: Wiley-VHCA; 2001. p. 3–14.
5. Tetko IV, Jaroszewicz I, Platts JA, Kuduk-Jaworska J. Calculation of lipophilicity for Pt(II) complexes: experimental comparison of several methods. J Inorg Biochem. 2008;102(7):1424–37.
6. Nasal A, Siluk D, Kaliszan R. Chromatographic retention parameters in medicinal chemistry and molecular pharmacology. Curr Med Chem. 2003;10:381–426.
7. Martel S, Guillarme D, Henchoz Y, Galland A, Veuthey J, Rudaz S, *et al.* Chromatographic approaches for measuring log P. In: Mannhold R, editor. Molecular drug properties. Measurement and prediction. Darmstadt: Wiley-VCH; 2008. p. 331–55.
8. Valko K. Application of high-performance liquid chromatography based measurements of lipophilicity to model biological distribution. J Chromatogr A. 2004;1037(1–2):299–310.
9. Boobbyer DN, Goodford PJ, Mcwhinnie PM, Wade RC. New hydrogen-bond potentials for use in determining energetically favorable binding sites on molecules of known structure. J Med Chem. 1989;32:1083–94.
10. Goodford PJ. A computational procedure for determining energetically favorable binding sites on biologically important macromolecules. J Med Chem. 1985;28:849–57.
11. Wade RC, Goodford PJ. Further development of hydrogen bond functions for use in determining energetically favorable binding sites on molecules of known structure. 2. Ligand probe groups with the ability to form more than two hydrogen bonds. J Med Chem. 1993;36:148–56.
12. Cruciani G, Mannhold R, Kubinyi H, Folkers G. Molecular interaction fields. Applications in drug discovery and ADME prediction. Zurich: Wiley-VCH; 2006.
13. Caron G, Ermondi G. Lipophilicity, polarity, and hydrophobicity. In: Testa B, van de Waterbeemd H, editors. Comprehensive medicinal chemistry, vol. 5. 2nd ed. Oxford: Elsevier; 2006. p. 425–52.
14. Caron G, Ermondi G. Calculating virtual log P in the alkane/water system $\left(\log P^{N}_{alk}\right)$ and its derived parameters $\Delta\log P^{N}_{oct-alk}$ and $\log D^{pH}_{alk}$. J Med Chem. 2005;48(9):3269–79.
15. Vistoli G, Pedretti A, Testa B. Partition coefficient and molecular flexibility: the concept of lipophilicity space. Chem Biodivers. 2009;6:1152–69.
16. Obach RS, Lombardo F, Waters NJ. Trend analysis of a database of intravenous pharmacokinetic parameters in humans for 670 drug compounds. Drug Metab Dispos. 2008;36(7):1385–405.
17. Berellini G, Springer C, Waters NJ, Lombardo F. *In silico* prediction of volume of distribution in human using linear and nonlinear models on a 669 compound data set. J Med Chem. 2009;52(14):4488–95.
18. Caron G, Ermondi G, Gariboldi MB, Monti E, Gabano E, Ravera M, Osella D. The relevance of polar surface area (PSA) in rationalizing biological properties of several cis-diamminemalonatoplatinum(II) derivatives. ChemMedChem. 2009;4((10):1677–85.
19. Platts J, Oldfield SP, Reif MM, Palmucci A, Gabano E, Osella D. The RP-HPLC measurement and QSPR analysis of logP(o/w) values of several Pt(II) complexes. J Inorg Biochem. 2006;100 (7):1199–207.
20. Heudi O, Mercier-Jobard S, Cailleux A, Allain P. Mechanisms of reaction of L-methionine with carboplatin and oxaliplatin in different media: a comparison with cisplatin. Biopharm Drug Dispos. 1999;20(2):107–16.
21. Coste F, Malinge JM, Serre L, Shepard W, Roth M, Leng M, *et al.* Crystal structure of a double-stranded DNA containing a cisplatin interstrand cross-link at 1.63Å resolution: hydration at the platinated site. Nucleic Acids Res. 1999;27(8):1837–46.
22. Coste F, Shepard W, Zelwer C. Description of ordered solvent molecules in a platinated decanucleotide duplex refined at 1.6Å resolution against experimental MAD phases. Acta Crystallogr Sect D. 2002;58:431–40.
23. Pastor M, Cruciani G, Watson KA. A strategy for the incorporation of water molecules present in a ligand binding site into a three-dimensional quantitative structure-activity relationship analysis. J Med Chem. 1997;40:4089–102.
24. Caron G, Nurisso A, Ermondi G. How to extend the use of grid-based interaction energy maps from chemistry to biotopics. ChemMedChem. 2009;4(1):29–36.
25. Pagliara A, Khamis E, Trinh A, Carrupt PA, Tsai RS, Testa B. Structural properties governing retention mechanisms on RP-HPLC stationary phase used for lipophilicity measurements. J Liq Chromatogr. 1995;18:1721–45.
26. McIntosh DP, Cooke RJ, McLachlan AJ, Daley-Yates PT, Rowland M. Pharmacokinetics and tissue distribution of cisplatin and conjugates of cisplatin with carboxymethyldextran and A5B7 monoclonal antibody in CD1 mice. J Pharm Sci. 1997;86 (12):1478–83.
27. Welink J, Boven E, Vermorken JB, Gall HE, van der Vijgh WJ. Pharmacokinetics and pharmacodynamics of lobaplatin (D-19466) in patients with advanced solid tumors, including patients with impaired renal of liver function. Clin Cancer Res. 1999;5 (9):2349–58.
28. Ishibashi T, Yano Y, Oguma T. Population pharmacokinetics of platinum after nedaplatin administration and model validation in adult patients. Br J Clin Pharmacol. 2003;56 (2):205–13.
29. Ehrsson H, Wallin I, Yachnin J. Pharmacokinetics of oxaliplatin in humans. Med Oncol. 2002;19(4):261–5.
30. Lombardo F, Obach R, Shalaeva MY, Gao F. Prediction of volume of distribution values in humans for neutral and basic drugs using physicochemical measurements and plasma protein binding data. J Med Chem. 2002;45:2867–76.
31. Lombardo F, Obach R, Shalaeva MY, Gao F. Prediction of human volume of distribution values for neutral and basic drugs. 2. Extended data set and leave-class-out statistics. J Med Chem. 2004;47:1242–50.